JOURNAL OF AIRCRAFT
Vol. 49, No. 5, September–October 2012

In Situ Velocity Measurements in the Near-Wake of a Ship Superstructure

Cody J. Brownell,* Luksa Luznik,* Murray R. Snyder,† and Hyung Suk Kang‡
U.S. Naval Academy, Annapolis, Maryland 21401
and
Colin H. Wilkinson§
Zenetex LLC, California, Maryland 20619

DOI: 10.2514/1.C031727

Velocity measurements in a ship airwake are obtained in situ aboard a 108 ft naval training vessel. The measurements and analyses are motivated by the need for validation data for airwake computational fluid dynamics simulations. Three-component anemometers are placed above the bow of the ship and at numerous locations above a flight deck at the stern of the ship. Data are presented for a direct headwind (nominally 0 deg wind-over-deck). The mean velocity field shows a clear structure to the flow, dominated by a recirculation region in the near-wake of a hangar-like backward-facing step. The location of this primary vortex and the reattachment point on the flight deck are estimated. Reynolds stresses are presented to quantify the turbulent fluctuations, which are required for the prediction of unsteady loading on rotorcraft operating in this environment. Significant anisotropy is measured in the wake, both within the primary vortex and in the far field. The peak Reynolds shear stress is located in the recirculation region, while the streamwise normal stress is found to increase with height throughout the measurement domain. Finally, auto- and two-point velocity correlations from the flight deck provide an estimate of flow scales, showing the potential influence of turbulence on piloted helicopter operations.

I. Introduction

THE launch and recovery of rotary-wing aircraft from naval vessels presents a formidable challenge. Difficulties may arise due to the motion of the flight deck, the turbulent airflow in the wake of the ship superstructure, and interactions between the ship, sea, and the aircraft. At present, launch and recovery envelopes are determined through extensive flight tests that involve dedicated underway testing and obtaining subjective inputs from experienced test pilots. These tests are expensive and potentially dangerous and do not always result in a complete flight envelope.

The development of tools that can reduce the need for launch and recovery flight tests is a priority for many navies around the world. A validated computational fluid dynamics (CFD) simulation of the airflow over a ship superstructure could help to greatly limit the number of flight tests required, reducing the risk and expense of flight-envelope determination. This may be done by identifying a priori, via prediction of both steady and unsteady vehicle loads, the approximate interface between safe and unsafe operating conditions. Flight test points may then be concentrated in these interface regions, and testing of conditions that are most likely unsafe need not occur. A simulation capable of predicting vehicle loading will require more than just computation of the airwake, as the vehicle dynamics and the rotor wake play an important role. Still, an accurate airwake prediction is a prerequisite for any complete simulation that is to be used for the determination of operating envelopes.

A number of groups are currently developing ship airwake simulations [1–4]. To be effective, these simulations are required to accurately predict a number of steady-state and transient features of the wake flow. In terms of the helicopter aerodynamics, flight envelopes are often limited either because of a lack of adequate control margin or because of excessive pilot workload required to maintain station over the flight deck. Although rotor-control margins can presumably be determined from knowledge of the mean flow, pilot workload arises from the unsteady, turbulent interactions between the rotorcraft and the wake. Prior research has shown that the frequency bandwidth that has the greatest effect on pilot workload is approximately 0.2 to 2 Hz [5]. Although this band is far below the highest frequencies one would expect to find in the flow, it still imposes a burden on simulations to accurately determine the size, location, and intensity of the most energetic turbulent eddies in the ship airwake.

Because of the complexity of a ship airwake flow and the importance of an accurate prediction, simulations must be thoroughly validated before they can be of full use. Validation data may take the form of either wind-tunnel measurements on a model ship or in situ data from measurements aboard a vessel at sea. In either case, validation must encompass a range of wind directions as well as both mean and turbulent quantities. In situ measurements of air velocities on surface ships are difficult and expensive, often requiring cooperation of the weather, and as a result no complete results are publicly available in the literature. Despite the challenges, both individual navies and cooperative programs between navies have attempted at sea measurements with varying success. Some of the difficulties in performing in situ measurements are described by Wilkinson et al. [6]. Measurements have typically used arrays of sonic anemometers mounted at fixed locations over the flight deck of a ship. Anemometers are capable of providing three orthogonal velocity components, but they are often limited in temporal resolution and must average over a measurement volume that is larger than the smallest eddies in the flow.

The other main challenge of in situ data collection has been data quantity. Simulations need to be validated over a relatively large parameter space, encompassing a range of wind speeds, wind directions, and measurement locations above and around the flight path of a rotorcraft. Sample sizes for each measurement point also

Received 1 November 2011; revision received 22 January 2012; accepted for publication 7 March 2012.

*Assistant Professor, Mechanical Engineering Department, 590 Holloway Road.
†Permanent Military Professor, Mechanical Engineering Department, 590 Holloway Road; also Captain, U.S. Navy.
‡Assistant Research Professor, Mechanical Engineering Department, 590 Holloway Road.
§Aerospace Engineer.

need to be large to accurately assess the full range of scales in the flow. In past measurement campaigns, measurement duration has been limited to several minutes due to a range of factors including the weather and the choice of test location. Ideally, individual data-collection runs would last much longer to allow for accurate computation of the lowest frequencies in the flow. In underway data from Kowal [7], discussed in a paper by Zan et al. [8], measurement with anemometers was limited to 30 s in duration, limiting the statistical significance of the results.

As a result of the challenges described previously, most experimental work has focused on laboratory measurements of the wake behind model ships in a wind tunnel. Wind-tunnel measurements have been useful in determining the basic topology of ship airwake flows. A series of studies by Rhoades and Healey [9], Healey [10], and Johns and Healey [11] provided some of the first quantitative experimental data on the characteristics of ship airwakes. They studied the flow over a 1:141 scale ship model in a wind tunnel with a simulated atmospheric boundary layer, using three-component hot-wire anemometers, with the goal of establishing an airwake database for use in future simulations. Velocity spectra and turbulence intensities are presented for flow at a yaw angle of 30 deg. More recently, Tinney and Ukeiley performed particle image velocimetry and flow visualization at $Re = 9000$ on a bare-hull wind-tunnel model described as a double backward-facing step [12]. A thorough description of the flow topology reveals a number of features, including a dominant horseshoe vortex immediately aft of the first step, and a sketch of the reattachment line on the deck below. They present mean-flow streamlines and single-point turbulent statistics, which are compared to prior results from both two-dimensional backward-facing step flows and separated flows over wall-mounted cubes. Work by Zan and Garry presents a similar flow topology for a simple frigate shape and includes turbulent energy spectra for velocity measurements over the flight deck [13]. Zan and Garry also present data suggesting a correlation length scale for turbulent eddies in this region [14].

One difficulty with wind-tunnel measurements is the inclusion and quantification of an atmospheric boundary layer. Work by Polsky [15] and a review by Zan [16] emphasize the dramatic differences between CFD simulations with and without an atmospheric boundary layer. The inclusion of a boundary layer changes not only velocity magnitudes but also the appearance and location of many dominant flow structures. A number of ship airwake investigations include a simulated boundary layer in the wind tunnel, but it remains a challenge to reproduce a realistic inflow in a laboratory setting. For in situ data, measurement of the incoming atmospheric flow profile is extremely difficult. Complete inflow assessment would require simultaneous velocity measurement at a number of elevations in a location where the ship's presence is not yet felt. Still, in situ measurement of the inflow will be valuable for defining boundary conditions for simulations and desired inflow conditions in the wind tunnel, and work on this is ongoing.

Another atmospheric flow where the boundary layer is important is in bluff-body flows, such as those over tall buildings. Wake descriptions are available in the literature from simulations of the flow over buildings [17] and from wind-tunnel experiments using wall-mounted cubes and prisms [18,19]. In these flows, the wake is typically dominated by a few large vortical structures, which may be stationary or may be shed periodically. Incoming turbulence typically results in enhanced mixing and entrainment, potentially modifying the flow separation and wake structure. Not surprisingly, the flight of a helicopter in the wake of tall buildings poses some similar challenges to helicopter flight in the ship airwake [20]. A review of bluff-body flows and their relationship to the ship airwake problem may be found in [21]. Although the research on bluff-body flows is of value in understanding the ship airwake flow, there are significant differences between the two cases. The geometry, high aspect ratio (length to beam), and independent motion of ships make their interactions with a boundary layer much more complicated than what is seen in the flow over a tall building. Furthermore, a ship airwake flow is distinguished by the irregular nature of the ship superstructure. Although tall buildings will often shed large vortical structures, the numerous appendages and small-scale features aboard a typical naval vessel breaks up most large structures and produces a qualitatively different flow in the near-wake region. Although the aircraft hangar typically found immediately forward of the flight deck presents a clean trailing edge, the effects of the upstream wake turbulence are still significant. The relatively low aspect ratio (height to beam) of a typical hangar also, by itself, precludes the existence of periodic vortex shedding.

Ideally, new ship airwake simulations will be validated with both in situ data and with wind-tunnel measurements, which offer control and repeatability. However, the lack of any published in situ data for comparison with either wind-tunnel or CFD data is a major concern. Wind-tunnel data alone cannot be used to validate CFD, especially considering potential issues with recreating the atmospheric boundary layer. Additional barriers to wind-tunnel validation will be found in future simulations that incorporate ship motion and ship–rotorcraft interactions.

This paper presents one part of a three-pronged effort aimed at understanding and predicting the air flow over the superstructure of Navy ships [22]. As a representative ship model, the U.S. Naval Academy (USNA) has use of a patrol craft (YP), a 108 ft long training vessel that is similar in configuration to a modern cruiser or destroyer. Using this platform, the airwake is assessed in three ways: through scale tests on a wind-tunnel model with matched Reynolds number [23], computationally using a monotone integrated large eddy simulation (MILES) method [24,25], and through in situ measurements aboard the ship, while underway in the Chesapeake Bay. The initial goal of the in situ measurements is to confirm the flow topology discussed earlier and to provide data on both mean and turbulent flowfield properties for CFD and wind-tunnel validation.

II. Experiment

A. Measurement Platform

The patrol craft (training), referred to as a YP, is a nonaviation surface ship used as a training aid for midshipmen at the U.S. Naval Academy. A YP (Fig. 1) measures 32.9 m (108 ft) in length, with an above-waterline height of 7.3 m (24 ft). Although several times smaller than a modern cruiser or destroyer (the Arleigh Burke class destroyer is 154 m in length), the vessel is similar in overall shape and likely large enough to experience a qualitatively similar airwake. Using the YP Craft as the ship platform for airwake assessment also allows matching of Reynolds numbers (up to wind-over-deck speeds of approximately 3.6 m/s) with experiments in a USNA wind tunnel. The YP craft used for these measurements was modified to accommodate the required instrumentation and to more closely resemble the shape of a cruiser or destroyer. The most substantial change was the addition of a 6.5 by 5.6 m flight deck on the aft end, and a modification to the aft superstructure to resemble the hangar on a modern destroyer. The hangar step height H is 1.50 m above the flight deck. A sketch of the modified vessel is shown in Fig. 2. Instrumentation consists of an array of three-component ultrasonic anemometers operating at 20 Hz, a GPS unit for ship location and velocity, and an inertial measurement unit for ship pitch and roll. Up to six anemometers were used for the experiments, including one instrument above the bow. All six anemometers are attached to a data packer, which allows for simultaneous data acquisition among all instruments.

B. Run Conditions

The data presented herein is for a single relative wind-over-deck (WOD) angle of 0 deg, a direct headwind, obtained over a number of days in the spring and summer of 2010. For data included here, WOD ranged from 5.5 to 13 m/s, with 10th and 90th percentiles of 6.09 and 10.09 m/s, respectively. The sea state for each underway was between 1 and 3, and ship pitch and roll never exceeded ± 3 deg. At these conditions, the flow Reynolds number based on ship length is on the order of 10^7.

With a direct headwind, a significant fraction of the WOD is due to ship speed, vice ambient winds. Ship speed for these measurements,

Fig. 1 Patrol craft YP 676, with a modified flight deck and aft hangar-like superstructure.

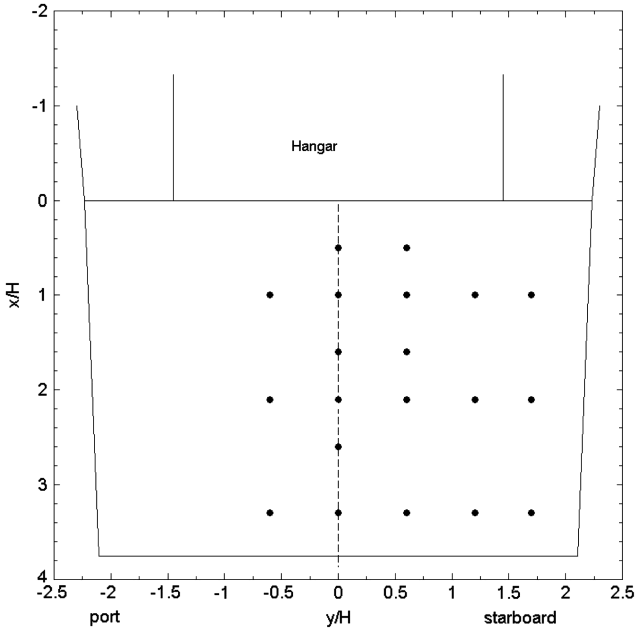

Fig. 3 Spatial arrangement of anemometers in the x–y (horizontal) plane. Dimensions are normalized with hangar height $H = 1.5$ m

which may be assumed constant, is about 4 m/s (8 kt), and thus linear ship motion contributes between 30 and 70% of the measured velocities. We anticipate that the ship speed affects both the incoming velocity profile and the overall velocity magnitude. However, the motion of the ship into the wind, at constant speed, has the effect of reducing variation in the shape of the incoming velocity profile compared to what one would see in a stationary case. Therefore, for this particular configuration, there may be more day-to-day consistency in the data than what one would expect from data taken at higher WOD angles with less relative ship motion.

With the present resources, the problem of short data streams and overall insufficient data quantity has been addressed. Typical data sampling (velocity measurements at a particular anemometer location and for a nominally fixed WOD angle) are 20 to 30 min. A number of runs have also been repeated to assess data repeatability, scaling, or when data quantity was deemed marginal. For the next analyses, any data patch with sustained deviation from the nominal 0 deg WOD by more than 5 deg is discarded, as is any patch where the bow velocity drops below 4 m/s. This filtering, combined with occasional equipment-related data dropouts, has only a small effect on the calculation of mean quantities but significantly reduces the length of continuous data streams for the analysis of large scale phenomena. Data stationarity was determined using a run test, as described in [26]. For the results presented here, data were found to be stationary for durations between 5 and 30 min. All mean and turbulent quantities presented are obtained over that averaging period.

The potential measurement locations are arranged in a grid over the flight deck, limited by the locations in which an anemometer may be rigidly mounted. Measurement locations over the flight deck are shown in Fig. 3. In the coordinate system used here, x is positive aft, y is positive to starboard, and z is positive up. In the horizontal (x–y) plane there are 20 potential measurement locations, each with 11 potential vertical (z) positions. Due to time constraints, this matrix is not fully populated. The data set contains 214 distinct measurement points in the wake, a number of which are repeat points from different days. Due to mounting inconsistencies, these repeat points may differ by up to 6 cm in terms of their actual measured location over the deck. In all data presented, the physically measured values are used to note instrument location. In z, the measurement heights vary between $z/H = 0.3$ and 1.4, where H (1.5 m) is the height from the flight deck to the top of the hangar structure. The number of data points in z varies from location to location, with generally more data available for points along the ship centerline. The data points are concentrated on the starboard side of the ship, as the flow is expected to be symmetrical for the case of a direct headwind. Several measurements on the port side, at $y/H = -0.5$,

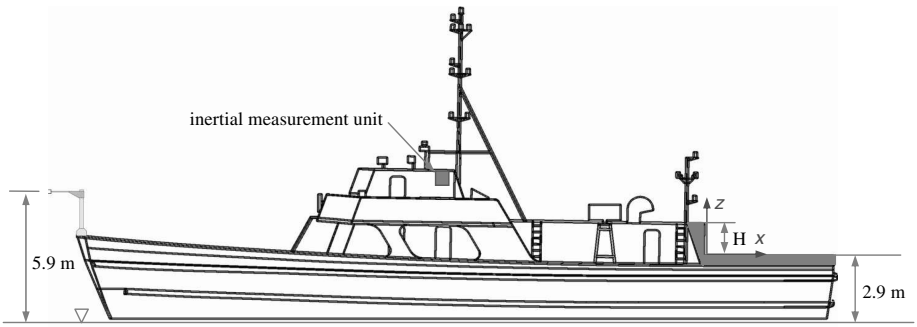

Fig. 2 Schematic of the modified YP. Hangar, flight deck, and location of bow anemometer are highlighted. The hangar height is $H = 1.5$ m, and the flight deck dimensions are length of 5.6 m and width of 6.7 m. The coordinate system used throughout is shown, with the origin at the ship centerline.

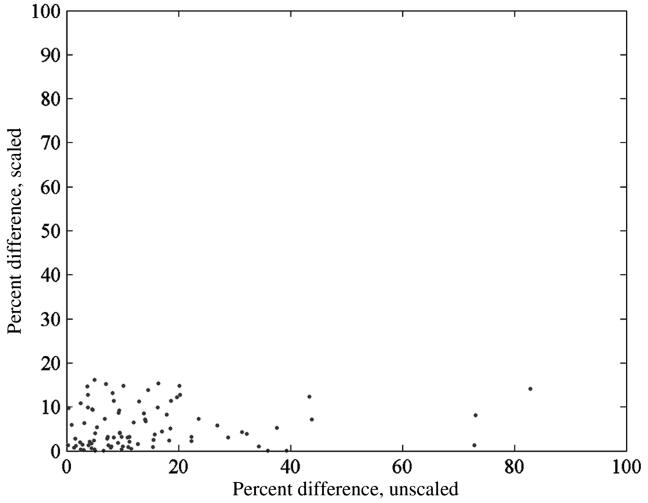

Fig. 4 Percent difference between mean velocities that share an interrogation region, before and after scaling by the mean bow velocity.

were obtained to confirm the symmetry assumption. A reference bow anemometer is located above and forward of the ship's bow to measure inflow conditions with minimal ship-related flow distortion [3]. The bow anemometer remains in place for all measurements and is located at $x/H = -18.953$ and $z/H = 2.065$.

III. Scaling and Repeatability

Incoming flow conditions vary significantly between data samples depending on the daily weather conditions (wind speed and direction, atmospheric pressure and temperature, and sea state) and the ship's operating conditions (engine speed and craft master experience.) Variations in the mean streamwise bow velocities between 5.34 and 12.11 m/s are observed over the entire data set. Even among data collected on a single day, significant variation can be observed. Data repeatability is tested qualitatively from two perspectives: first through examination of the mean velocity above the flight deck, and second through examination of the Reynolds shear stresses. During testing, velocity measurements from the same location were frequently recorded on different days, which resulted in different atmospheric conditions. (In practice, the first data-collection run on a given day would often repeat the last data run on the previous day.) In the data set, there are 198 points that share the same interrogation region as another point. Of these points, 90 have a mean velocity greater than 0.75 m/s and are used for repeatability testing. Figure 4 shows the percent difference of data points sharing an interrogation region both before and after scaling by the mean bow velocity. Before scaling, mean velocity from data pairs sharing an interrogation region varies from less than 1% to a maximum of 82%, with a median value of 10%. When these velocities are scaled by the mean bow velocity, the results are much more consistent; variation in the mean velocity ranges from 0 to 16%, with a median value of 3.8%.

As an additional validation for the use of U_∞ as a velocity scale, a weighted joint probability density function (JPDF) of the streamwise and vertical velocity fluctuations is employed to analyze the turbulence structures generating high Reynolds shear stress. The JPDF, $P(u, w)$, is defined as

$$1 = \int_{-\infty}^{\infty} P(u, w)\, \mathrm{d}u\, \mathrm{d}w \tag{1}$$

where u and w are the fluctuating velocity components in the x and z directions, respectively. Figure 5a shows the contour lines of the weighted JPDF measured at $x/H = 2.15$, $y/H = 0$, and $z/H = 0.67$. The dashed and solid contour lines indicate the measurements for $U_\infty = 6.07$ and 7.56 m/s, respectively. The first and third quadrants contribute to the negative Reynolds shear stress, and are not associated with the turbulence structures, but the second and fourth quadrants are expected to provide a characterization of the flow turbulence. As shown in Fig. 5a, there is considerable difference between the solid and dashed contour lines, and vastly different turbulent structures from the two data sets may be expected. However, when the velocity fluctuations are normalized with the corresponding mean streamwise bow velocities, there is qualitative agreement between the two data sets, as shown in Fig. 5b. Therefore, these analyses indicate that scaling with the streamwise mean bow velocity is a reasonable assumption over small changes in flow Reynolds number. The remaining disagreement is potentially due to a number of factors, including differing atmospheric conditions.

IV. Results

A. Mean Velocities and Flow Structure

The mean streamwise and vertical velocity components over the flight deck are shown in Fig. 6. Note that, in the coordinate system used here, x is positive in the streamwise direction and z is positive up. Velocities from each data-collection run are scaled by the mean streamwise bow velocity for that run, as discussed in Sec. III. The streamwise bow velocity is also shown for comparison in each figure. Instrument locations in all three coordinates are independently measured before each data run, and variability between nominally identical locations is less than $0.04H$ (6 cm). In Fig. 6 the anemometer positions in x and z are plotted exactly, whereas the y planes have a small thickness that allows inclusion of data points that fall slightly to one side or the other of the plane.

Data is shown for five planes that step uniformly athwartships. One data plane (a) is located on the port side, $y/H = -0.6$, one (b) at the centerline, $y/H = 0.0$, and three (c–e) on the starboard side of the vessel at $y/H = 0.6$, 1.2, and 1.7, respectively. Planes a and c are

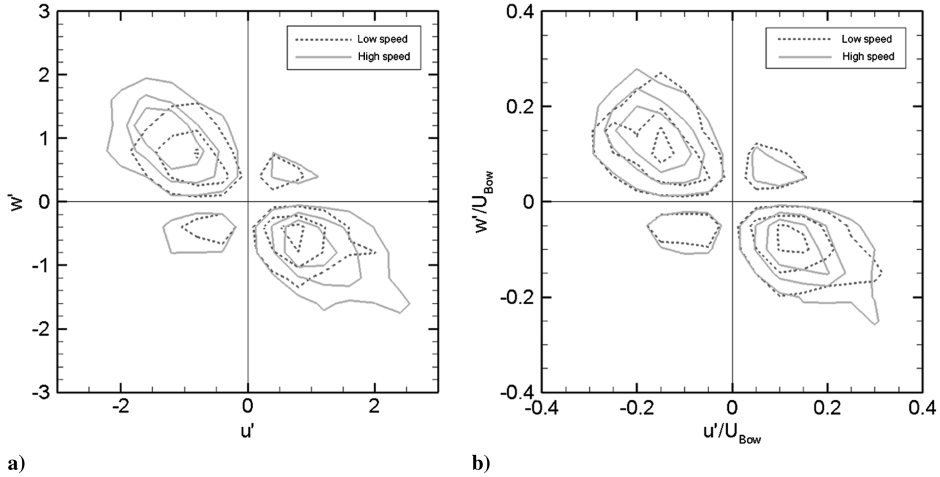

Fig. 5 JPDFs of the streamwise and vertical velocity fluctuations in the flow, a) presented as raw data and b) scaled by the mean streamwise bow velocity.

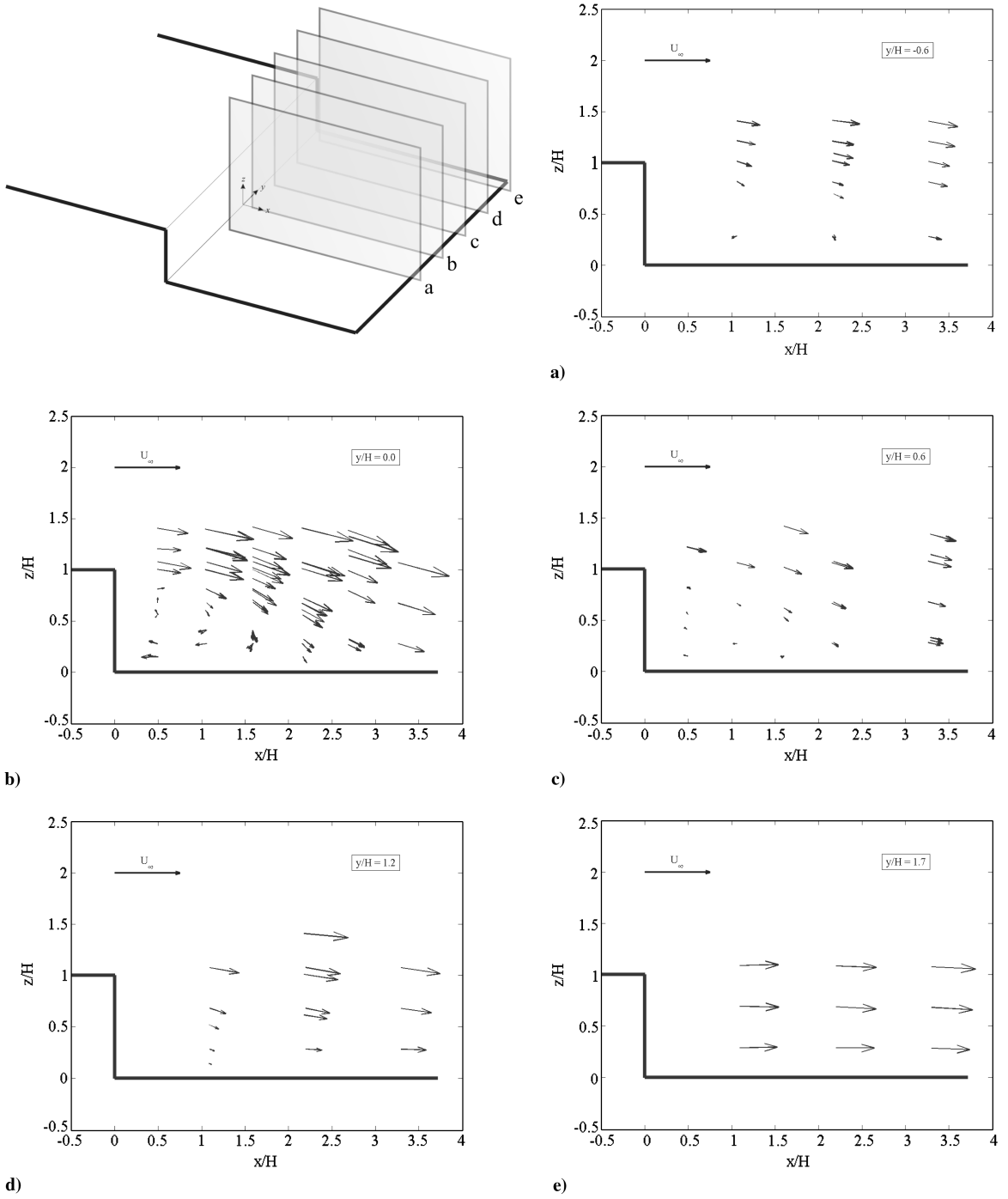

Fig. 6 Mean velocity over the flight deck in the streamwise plane. Velocities are scaled by the mean streamwise bow velocity, shown in each figure for reference. From the centerline velocity (b), the recirculation behind the hangar structure is visible.

symmetric about the ship centerline, and the measured velocities are likewise consistent with each other. Figure 7 shows the mean velocity from these two planes of symmetry plotted on the same axes.

Overall flow structure is generally consistent with that described by other authors from wind-tunnel measurements and numerical simulations. The dominant feature is a large recirculation zone immediately aft of the hangar structure, similar to the recirculation documented by Rhoades and Healey [9]. At the centerline, the height of the vortex core is slightly above the midpoint of the hangar, estimated to be around $z/H = 0.6$. Aft of the recirculation zone, the separated flow reattaches to the flight deck. The stagnation point designating the reattachment, again at the centerline, is estimated to be between $x/H = 1.5$ and $x/H = 2.0$. The parameters that define the location of the primary flow structure, that being the recirculation zone, should be consistent for all experiments and simulations that use this flow geometry, provided that the Reynolds number is sufficiently high [27,28]. To a certain extent, this is affirmed by the clarity of the structure in Fig. 6, itself determined from measurements with varying inflow velocity.

Outside of the main recirculation, there is significant downwash as the air moves through the low-pressure zone in the wake of the entire ship superstructure (including both the hangar and the pilot house further upstream). Velocity magnitudes also increase away from the centerline but remain well below the bow velocity at all points over the flight deck.

Mean velocities in the y–z plane, at a distance $x/H = 1.1$ from the hangar surface, are shown in Fig. 8. The aspect ratio of the hangar face, approximately 4.3:1, is not to scale in the figure. This slice is

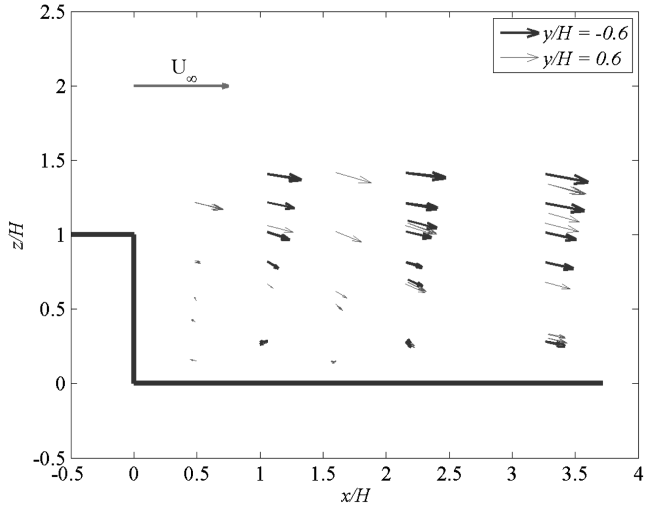

Fig. 7 Comparison of mean velocity on symmetrical planes.

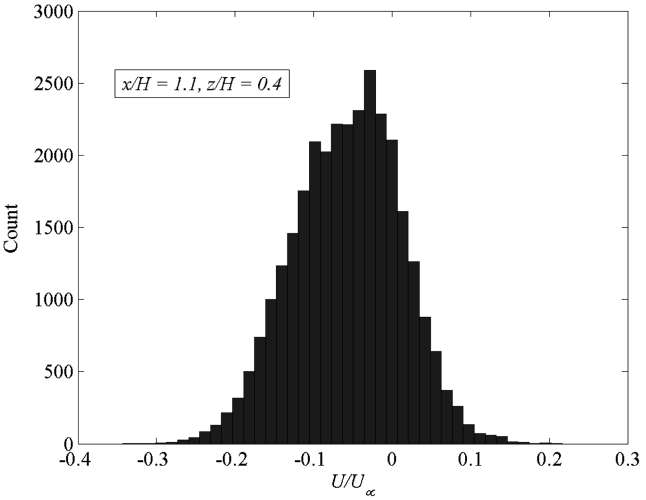

Fig. 9 Histogram of the streamwise velocity component from a single point over the flight deck. This point is located in the primary recirculation region and has a negative (backward) mean velocity.

within the main recirculation zone, which can be confirmed by a comparison with Fig. 6b. Notice again the overall downwash and the mean inflow toward the centerline through at least $y/H = 1.2$.

As with most other ship airwake studies, no periodic von Kármán vortex shedding is observed. This is primarily due to the aspect ratio (height to width) of the ship superstructure, which would need to be much larger for this to be a possibility. The experiments by Tinney and Ukeiley [12] show no periodicity even with a bare-hull model and a uniform inflow. In the near-wake, there is an irregular buildup and release of vorticity, resulting in a flow structure that is clear (i.e., from the mean profiles) but not necessarily visible in every snapshot of the flow. Figure 9 shows a histogram of velocity at a point within the recirculation region with mean reverse flow. The point is located at $x/H = 1.1$, $y/H = 0$, and $z/H = 0.4$, and the distribution is of the streamwise velocity component. Despite being located well within the recirculation zone, the streamwise velocity at this point is negative only 79% of the time. A positive velocity here indicates that, at that time, the vortex has either disappeared or moved significantly. Histograms of velocity at other points in the wake show a similar distribution to Fig. 9. Besides the hangar shape, the flow unsteadiness is influenced by both upstream wake turbulence and by the atmospheric boundary layer. The effects of upstream wake turbulence are an important consideration for wind-tunnel testing of ships because the degree of detail to include in a wind-tunnel model must be determined. An atmospheric boundary layer is likely to influence both the position of the main flow features and the unsteady characteristics of the flow. Similar to what is observed in the flow over surface-mounted cubes [19], one may expect to see a larger and higher main vortex, and a different reattachment point, from simulations that do not include any mean shear in the inflow. The relative influences and interaction between atmospheric turbulence and turbulence generated from the flow over the forward ship superstructure are unknown.

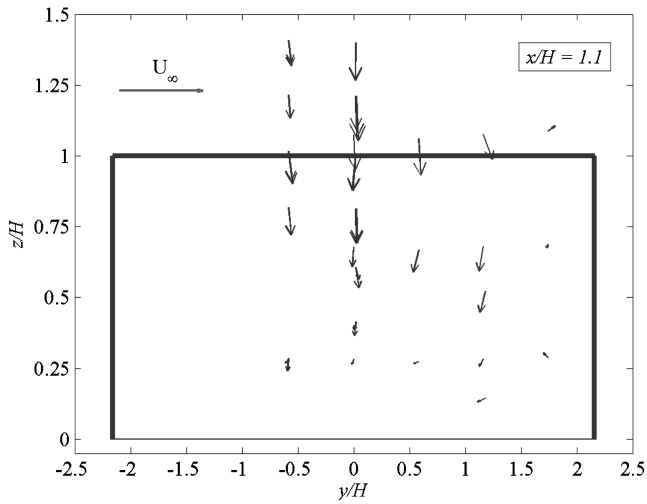

Fig. 8 Mean velocity in the y–z plane, at position $x/H = 1.1$ aft of the hangar. The rectangle depicts the hangar structure as would be seen from the aft of the deck, looking forward.

B. Turbulence Metrics

An assessment of flow turbulence is necessary for any ship airwake simulation used for flight-envelope determination. Not only do the "static" large-scale features of a ship airwake fluctuate in position and strength, but many of the smaller, intermittent turbulent eddies are strong enough to affect helicopter performance and pilot workload. Atmospheric simulations for fixed-wing aircraft typically employ Taylor's hypothesis to create a stationary flowfield that the aircraft traverses. This is inappropriate for many rotorcraft simulations, and particularly for simulations involving the launch and recovery of rotorcraft [29]. For the ship airwake/helicopter flowfield, the mean advection velocity of the air is possibly several times larger than the velocity of the helicopter fuselage, precluding the use of a stationary turbulent field. An uncoupled simulation of aerodynamic loading on a rotorcraft must therefore include, at a minimum, a complete statistical description of the flow. The influence of turbulence on rotor thrust is also an active area of investigation [30], requiring similar verification data.

Although a number of metrics may be used for CFD validation, the most important quantities are those that may be used as inputs to rotorcraft dynamic models. Despite advances in computing, fully coupled, real-time, predictive Navier–Stokes-based CFD simulations of the ship/helicopter dynamic interface will not be available in the near term [31]. Airwake simulations that now or in the future incorporate helicopter flight may model the airwake-rotorcraft interaction using a number of different techniques [29]. There is debate over the relative merits of modeling the interaction using time-accurate wake simulations, requiring a large amount of data, or using stochastic models, which are simpler but at the cost of lost flowfield information [32]. The stochastic models may quantify the fluctuating velocities using an autocorrelation function, a power spectral density approach, or a number of other statistical measures.

The analyses herein may be used for validation and assessment of turbulence models as well as for broad guidance in the development of new modeling techniques. We assess the turbulent flow structure in two ways: using autocorrelations and two-point spatial correlations of the measured velocity, as well as Reynolds stress calculations. Reynolds stresses, equivalent to the integral of the energy spectra, are

useful for identifying turbulent energy content, local flow structure, and isotropy. Put another way, the Reynolds stresses describe the intensity of the turbulent fluctuations in the wake, and the correlations describe the spacing of the same fluctuations.

The streamwise (R_{uu}) and vertical (R_{ww}) normal Reynolds stresses are shown as a function of height over deck in Figs. 10 and 11, respectively. All data are from the centerline, and four different streamwise locations, $x/H = 1.1, 1.6, 2.2$, and 2.7, are shown. These Reynolds stresses are the product of the fluctuating component of the velocity (e.g., $u = U - \bar{U}$) normalized by the square of the streamwise bow velocity:

$$R_{ij} = \overline{u_i u_j}/U_\infty^2 \tag{2}$$

where the overbar denotes averaging. The vertical line in the figure designates $z/H = 1$, equivalent to the hangar height immediately forward of the measurement region. The average velocity is determined by computing the mean velocity over a 15 s window surrounding the point of interest to damp out large-scale variance due to, e.g., shifting winds or craftmaster steering.

A general trend of increasing stress with height is observed, particularly with R_{uu}. This trend becomes slightly more pronounced as x/H increases, corresponding to a move away from the recirculation zone and toward regions with higher local mean velocity. An interesting comparison is found with the wind-tunnel measurements from Tinney and Ukeiley [12], who also present Reynolds shear stress components for a 0 deg yaw flow. On a bare-hull ship model, a maximum streamwise normal stress was found to sit below the hangar step height, roughly corresponding to the center of the recirculation zone. In magnitude, their maximum measured normal stress, calculated using Eq. (2), is approximately 0.063, which is slightly lower than the maximum values presented here. Unlike the present observations, they found R_{uu} to decrease significantly for locations above the step and out of the primary wake. This discrepancy can be partially explained by the differences in geometry between their wind-tunnel model and the present ship. On the YP, there is a significant superstructure above the hangar step, albeit several meters upstream. For a direct headwind, the flow moving over the top of the hangar already has residual turbulence from being in the wake of the pilot house. Although this explanation is sensible, another important factor is the amount of turbulence at the inflow. On the YP, a significant streamwise Reynolds stress component was measured by the bow anemometer: $R_{uu} = 0.007$, at a height of $z/H = 2.065$. Although the value of R_{uu} at the bow is less than the peak values in the wake, it is much higher than what is found in the far field in a laboratory flow without background turbulence. Last, low-frequency variations in inflow velocity, which would be absent in the wind-tunnel measurements, would result in increased normal stresses in regions where the stress would otherwise be low.

The vertical component of the normal Reynolds stress, R_{ww}, is generally smaller than R_{uu}, especially at larger z/H. Although there is less change in R_{ww} with elevation as compared to R_{uu}, it appears that the stresses measured above the hangar height are at least as large as those measured inside the recirculation region. A possible explanation for this is the same as that previously provided for R_{uu}. A quantitative comparison of the normal components of the Reynolds stress show significant anisotropy in the wake. Isotropy has important implications for flow-modeling techniques and for a number of rotorcraft models. An isotropy ratio I can be defined by the ratio of the streamwise and vertical rms velocities and is also equal to the square root of the normal stress ratio:

$$I = u_{\text{rms}}/w_{\text{rms}} = (R_{uu}/R_{\text{ww}})^{1/2} \tag{3}$$

In the present domain, this varies between a low of 0.9 and a high 2.1, with values generally increasing with both y/H and z/H. This range is consistent with numerous measurements from backward-facing step flows. The values less than unity, where vertical

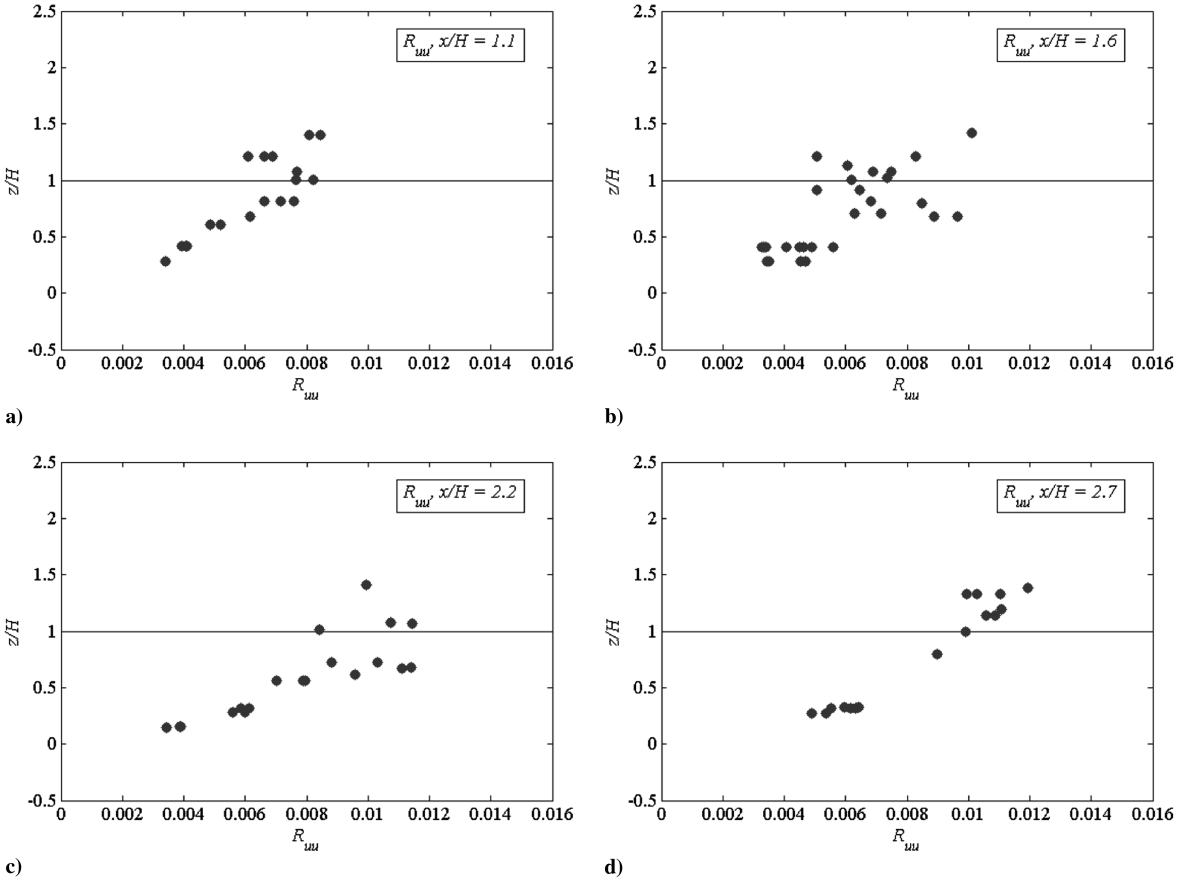

Fig. 10 Streamwise (R_{uu}) normal stresses as a function of height over deck. All data are from the ship centerline, and the vertical line marks the location of the top of the hangar. Values are found to increase with increasing height, including points that are above the hangar height.

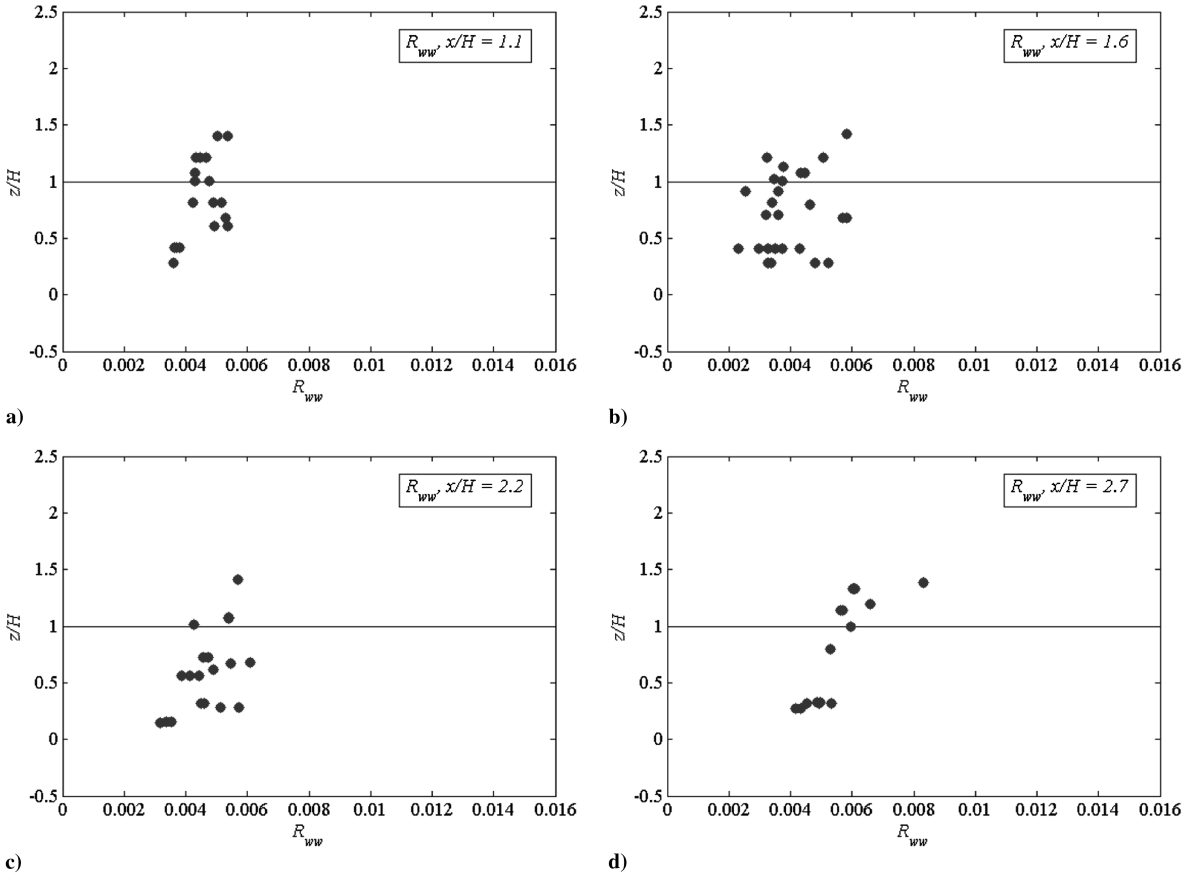

Fig. 11 Vertical (R_{ww}) normal stresses as a function of height over deck. All data are from the ship centerline, and the vertical line marks the location of the top of the hangar. Values of R_{ww} are lower than R_{uu} and do not appear to increase significantly with height.

fluctuations are larger than horizontal fluctuations, are found in regions with a significant mean vertical velocity component: on either side of the primary vortex or close to the deck near the reattachment point.

Figure 12 shows the Reynolds shear stress R_{uw} along the centerline of the flight deck and at the same four stations as before. Unlike the normal stresses, where the maximum values were found on the upper boundary, a maximum shear stress is found at approximately $z/H = 0.7$ for the three measurement stations closest to the hangar. This is near (slightly above) the center of the main recirculation and is indicative of a strong velocity gradient in the region. The differences in the trends between R_{uu} and R_{uw} are interesting and unusual for a wake flow. One possible explanation is that the difference is due to varying inflow conditions. Large, low-frequency fluctuations in the incoming velocity would result in an increased streamwise normal stress in the more exposed flow regions. The shear stress, however, would not necessarily increase with these inflow changes unless they are also accompanied by additional transient eddies. The recirculation immediately behind the hangar is a stable feature, largely independent of flow Reynolds number and the low-frequency behavior of the inflow, and therefore the turbulent statistics from that region are more typical of other wake flows. A rigorous test of this hypothesis would require a spectral analysis on a longer data series, without the conditional sampling employed here.

Figure 13 shows the turbulence intensity (TI) calculated here from the Reynolds stresses:

$$\mathrm{TI} = \sqrt{\frac{1}{3}(R_{uu} + R_{vv} + R_{ww})} \tag{4}$$

The turbulence intensity is a measure of an rms velocity fluctuation divided by a mean velocity. The mean bow velocity is used rather than a mean local velocity to remain consistent with the rest of the analysis. The distribution of the turbulence intensity is similar in appearance to R_{uu}, the largest of the Reynolds stress components, and is presented here to facilitate comparisons with other data.

C. Velocity Correlations

Velocity correlations from measurements over the flight deck provide a direct estimate of the relevant length scales in the flow. An autocorrelation function may be defined as

$$\rho_i = \frac{\overline{u_i(t)u_i(t+\tau)}}{\overline{u_i(t)^2}} \tag{5}$$

where t is time, τ is the time since t, and the overbar again denotes averaging. Assuming the flow consists of a range of turbulent structures that are advected downstream, then the autocorrelation indicates, in a broad sense, how long a particular eddy is expected to reside at a particular point in the flow. Velocities at different points within the same eddy are likely to be correlated, whereas velocities at different points within different eddies are likely to be independent. The autocorrelation is a function of time and is typically multiplied by a characteristic flow velocity to estimate a length scale (i.e., the size of a coherent structure or eddy). Because these measurements are from the wake, the natural choice of velocity scale (the bow velocity U_∞) may not be the appropriate local advective velocity. The local mean velocities over the flight deck are much smaller than the bow velocity, but they also differ significantly from one point on the deck to another. With no other suitable advective velocity, the autocorrelations presented here are normalized using the bow velocity U_∞ and the hangar height H. However, because of these issues, the autocorrelations are not directly comparable to the cross correlations presented later.

Velocity autocorrelations over the flight deck are shown in Fig. 14, at both $z/H = 0.4$ (Fig. 14a), directly behind the hangar structure, and at $z/H = 1.1$ (Fig. 14b), which is slightly above the top of the hangar. Both plots are from the ship centerline ($y/H = 0$) and at

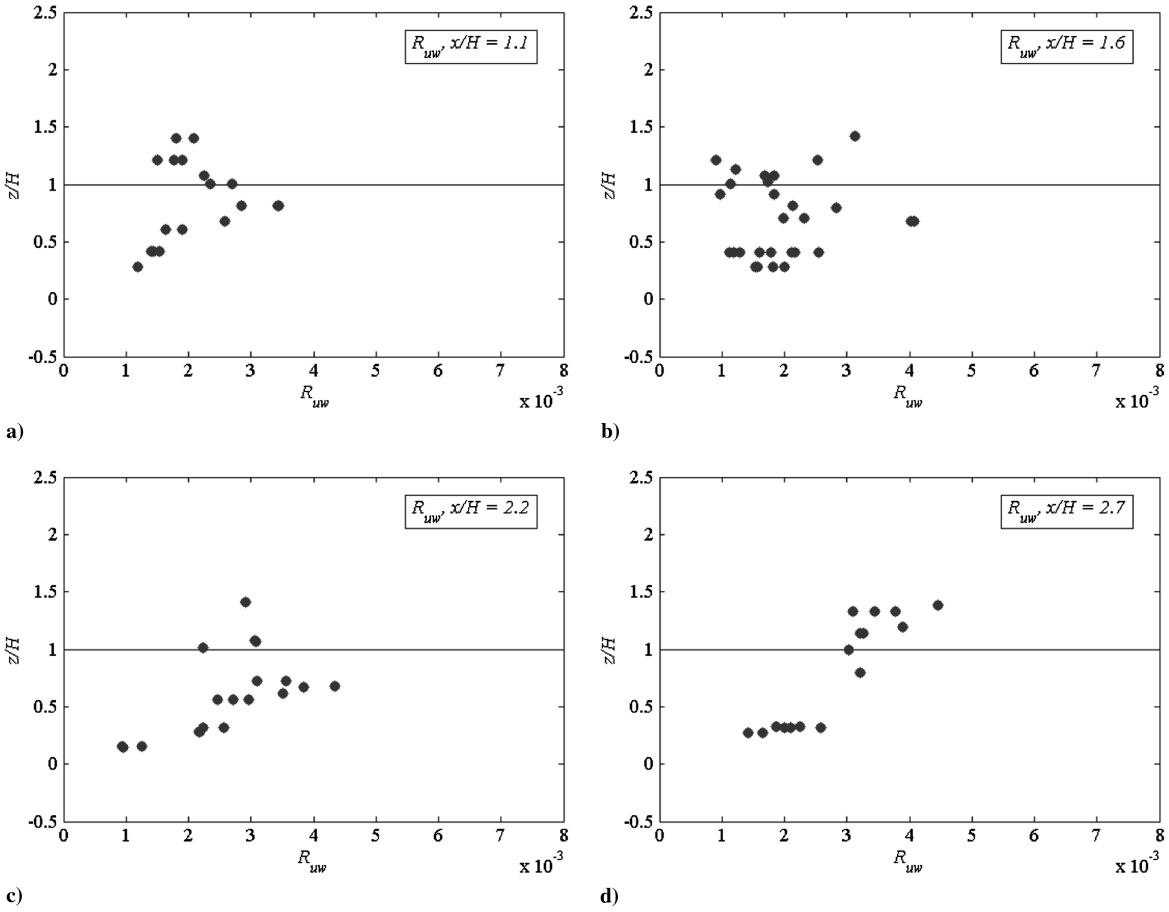

Fig. 12 Reynolds shear stresses R_{uw} along the centerline at four stations: $x/H = 1.1$, 1.6, 2.2, and 2.7. For the three stations closest to the hangar, the largest shear stress is found at a height below the top of the hangar step.

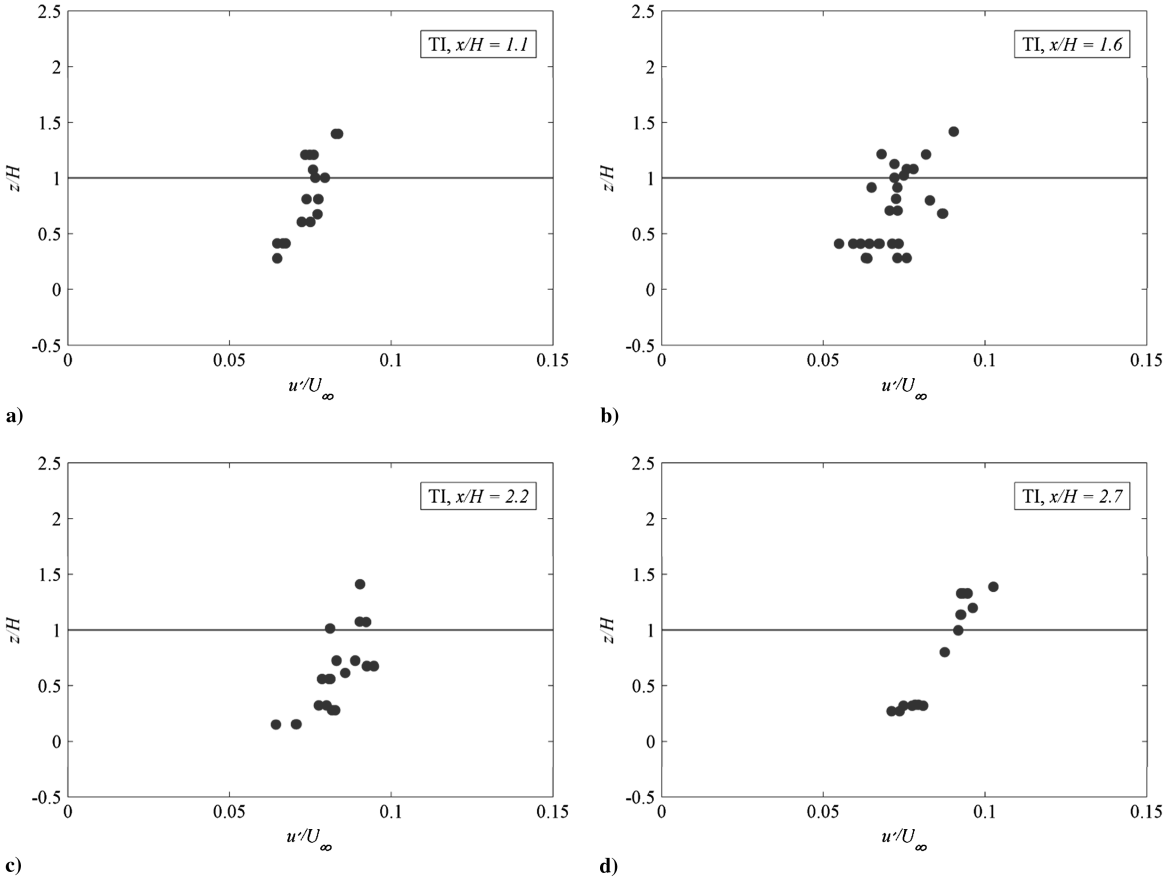

Fig. 13 Plots of TI along the centerline of the flight deck.

$x/H = 1.6$. The solid line is ρ_u, the dashed line is ρ_v, and the dash-dot line is ρ_w. The mean bow velocity for the subset of data presented in this figure is $U_\infty = 5.0$ m/s. In Fig. 14a, the correlations in the x (streamwise) and z (vertical) directions are larger than those in y, due to the location of this interrogation region within the recirculation zone, where the mean flow is rotating in the x–z plane. The correlations have all fallen off below $\rho = 0.3$ by $\tau U_\infty/H = 5$, which corresponds to approximately 1.5 s of residence time. This time easily falls within the range of frequencies estimated to impact pilot workload most significantly. In Fig. 14b, from measurements above the top of the hangar, a decline in correlation lengths is seen in all components. In particular, R_{ww} has decreased significantly compared to R_{uu} due to the fact that this is no longer in the recirculation zone. The turbulence in this region is due to atmospheric conditions and the upstream ship superstructure, but it does not have anything like the large eddies that are seen in the near-wake of the hangar.

An alternative measure of the size of turbulent structures is the two-point cross correlation of the velocity, calculated here as

$$\rho_{12} = \frac{\overline{u_1(t)u_2(t)}}{[u_1(t)]^2[u_2(t)]^2{}^{1/2}} \tag{6}$$

Unlike the autocorrelation, this is explicitly a function of length (i.e., the distance between interrogation points) and is therefore normalized by a length (the hangar height) without need for an advective velocity. Figure 15 shows a comparison of two-point velocity correlations, at $x/H = 1.6$ and $y/H = 0$. The circles, squares, and triangles represent the u, v, and w velocity components, respectively. In each case, u_1 is the velocity nearest the flight deck ($z/H = 0.2$) and u_2 is the velocity at a distance r/H above u_1, where r is the distance between the interrogation points. It is important to note that spatial homogeneity, often assumed when computing two-point statistics, is not present here. As with the autocorrelations, the correlations in the x and z directions are noticeably larger than in the y direction. The correlation in z is actually larger than in x over most separation distances, probably due to the particular placement of this

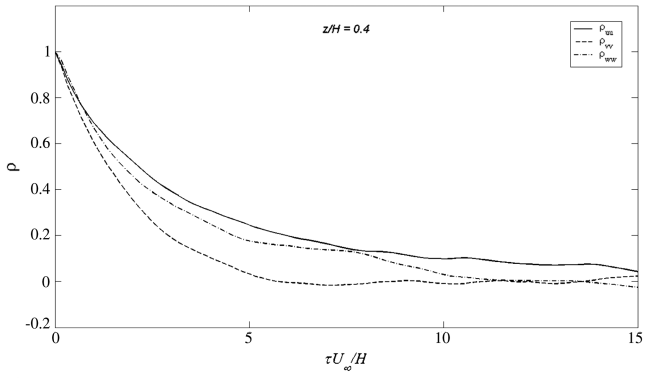

a)

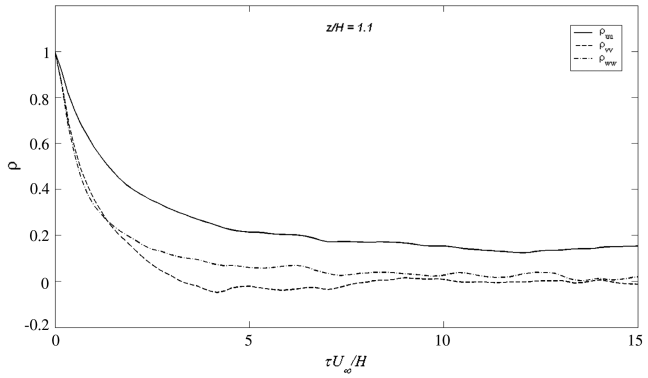

b)

Fig. 14 Velocity autocorrelations in the ship wake, at a) $z/H = 0.4$ and b) $z/H = 1.1$. Both plots are from points along the ship centerline ($y/H = 0$) and at $x/H = 1.6$.

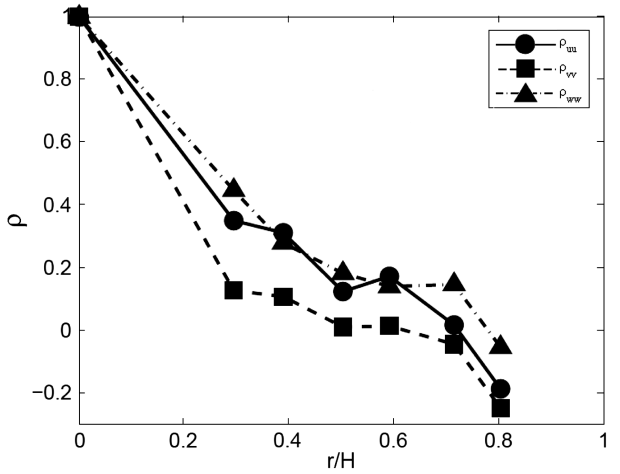

Fig. 15 Two-point cross correlation in the wake, at $x/H = 1.6$ and $y/H = 0$, where r is the distance between interrogation points. All correlations are between velocity at a height of $z/H = 0.2$ and a second elevation higher on the deck.

measurement with respect to the wake. The position $x/H = 1.6$ is at the tail end of the recirculation region, where the magnitude of W is often larger than the magnitude of U. Combined with the fact that the separation distance r is measured in the vertical direction, this observation is not surprising. At least one component of the correlation remains above $\rho = 0.3$ through approximately $r/H = 0.4$, indicating that many of the eddies have a characteristic size that is quite a bit smaller than the hangar height H. As stated before, this cannot be directly compared to the autocorrelation because of the lack of an appropriate advective velocity. However, the turbulent length scales are in a range that may affect helicopter operations, through either unsteady fuselage loading or rotor–turbulence interactions.

V. Conclusions

In situ measurements of air velocity in the near-wake of a 108 ft naval vessel are presented for a case of a 0 deg headwind. The flow is found to separate over a hangar-like backward-facing step, with a persistent recirculation zone immediately aft of the step face. The flow reattaches to the flight deck downstream, in the range $x/H = 1.5$ to $x/H = 2.0$. Calculation of the Reynolds stresses in the wake show anisotropy both in the near-wake immediately over the deck and at points above the top of the hangar. The vertical distribution of the shear stress component R_{uw} shows a maximum value below the height of the hangar, whereas the normal stress component R_{uu} continues to increase through at least a height of $z/H = 1.4$. Both auto- and two-point spatial correlations in the wake provide estimates of the sizes of turbulent structures in the wake. In both cases, scales were found to fall directly within the range assumed to have the largest impact on rotorcraft operations.

The objective of this work is to provide validation data for ship airwake simulations and wind-tunnel measurements. As a baseline case, the measurements herein are for a nominal headwind of 0 deg from the bow, $+/-5$ deg. Although validation at this yaw angle is required, evidence suggests that flow structure can change drastically as the direction of the wind over deck changes. The ability of a simulation or experiment to capture these changes and the points at which they occur is as important as reproducing the features for a given flow condition. Future work at the U.S. Naval Academy will involve flow mapping over a range of inflow conditions, where the inflow is comprised of ambient wind direction, ship speed and heading, and a more complete description of the atmospheric boundary layer.

Acknowledgments

Support from the Office of Naval Research through the Young Investigator Program (Principal Investigator (PI): Murray R. Snyder)

is gratefully acknowledged. The authors would also like to recognize the invaluable contributions of John Burks and Joshua Shishkoff to this paper and to the U.S. Naval Academy ship airwake program.

References

[1] Polsky, S., Imber, R., Czerwiec, R., and Ghee, T., "A Computational and Experimental Determination of the Airflow Around the Landing Deck of a U.S. Navy Destroyer (DDG): Part 2," 37th AIAA Fluid Dynamics Conference and Exhibit, Miami, FL, AIAA Paper 2007-4484, June 2007.

[2] Sezer-Uzol, N., Sharma, A., and Long, L. N., "Computational Fluid Dynamics Simulations of Ship Airwake," *Proceedings of the Institution of Mechanical Engineers*, Vol. 219, No. 5, 2005, pp. 369–391. doi:10.1243/095441005X30306

[3] Snyder, M. R., Shishkoff, J. P., Roberson, F. D., McDonald, M. C., Brownell, C. J., Luznik, L., et al., "Comparison of Experimental and Computational Ship Air Wakes for YP Class Patrol Craft," *ASNE Launch and Recovery Symposium*, Arlington, VA, American Society of Naval Engineers Paper ADA529728, 2010.

[4] Forrest, J. S., and Owen, I., "An Investigation of Ship Airwakes Using Detached-Eddy Simulation," *Computers and Fluids*, Vol. 39, No. 4, 2010, pp. 656–673. doi:10.1016/j.compfluid.2009.11.002

[5] McRuer, D. T., "Interdisciplinary Interactions and Dynamic Systems Integration," *International Journal of Control*, Vol. 59, No. 1, 1994, pp. 3–12. doi:10.1080/00207179408923067

[6] Wilkinson, C. H., Zan, S. J., Gilbert, N. E., and Funk, J. D., "Modelling and Simulation of Ship Air Wakes for Helicopter Operations—A Collaborative Venture," *RTO AVT Symposium on Fluid Dynamics Problems of Vehicles Operating near or in the Air-Sea Interface*, Amsterdam, The Netherlands, 1998.

[7] Kowal, H. J., "Wind Over Deck Survey and CH-124A/CPF Flight Deck Qualification Trials," *Flight Dynamics Technical Memorandum FD TM 91/05, Aerospace Engineering Test Establishment*, Department of National Defense, Canada, Dec. 1991.

[8] Zan, S. J., Syms, G. F., and Cheney, B. T., "Analysis of Patrol Frigate Air Wakes," *Symposium on Fluid Dynamics Problems of Vehicles Operating Near or in the Air-Sea Interface*, Amsterdam, The Netherlands, Oct. 1998.

[9] Rhoades, M. M., and Healey, J. V., "Flight Deck Aerodynamics of a Nonaviation Ship," *Journal of Aircraft*, Vol. 29, No. 4, 1992, pp. 619–626. doi:10.2514/3.46210

[10] Healey, J. V., "Establishing a Database for Flight in the Wakes of Structures," *Journal of Aircraft*, Vol. 29, No. 4, 1992, pp. 559–564. doi:10.2514/3.46202

[11] Johns, M. K., and Healey, J. V., "The Airwake of a DDG-963 Class Destroyer," *Naval Engineer's Journal*, Vol. 101, No. 3, 1989, pp. 36–42. doi:10.1111/j.1559-3584.1989.tb02184.x

[12] Tinney, C. E., and Ukeiley, L. S., "A Study of a 3D Double Backward-Facing Step," *Experiments in Fluids*, Vol. 47, No. 3, 2009, pp. 427–438. doi:10.1007/s00348-009-0675-9

[13] Zan, S. J., "Surface Flow Topology for a Simple Frigate Shape," *Canadian Aeronautics and Space Journal*, Vol. 47, No. 1, 2001, pp. 33–43.

[14] Zan, S. J., and Garry, E. A., "Wind Tunnel Measurements of the Airwake Behind a Model of a Generic Frigate," National Research Council Rept. IAR-LTR-AA-13, June 1994.

[15] Polsky, S. A., "CFD Prediction of Airwake Flowfields for Ships Experiencing Beam Winds," *21st AIAA Applied Aerodynamics Conference*, Orlando, FL, AIAA Paper 2003-3657, June 2003.

[16] Zan, S. J., "On Aerodynamic Modelling and Simulation of the Dynamic Interface," *Proceedings of the Institution of Mechanical Engineers*, Vol. 219, No. 5, 2005, pp. 393–410. doi:10.1243/095441005X3031510.1243/095441005

[17] Kareem, A., "Bluff Body Aerodynamics and Aeroelasticity: A Wind Effects Perspective," *Journal of Wind Engineering and Industrial Aerodynamics*, Vol. 7, No. 1, 2010, pp. 30–74.

[18] Uffinger, T., Becker, S., and Ali, I., "Vortex Dynamics in the Wake of Wall-Mounted Cylinders: Experiment and Simulation," *15th International Symposium on Applications of Laser Techniques to Fluid Mechanics*, Paper 1741, Lisbon, Portugal, July 2010.

[19] Castro, I. P., and Robins, A. G., "The Flow Around a Surface-Mounted Cube in Uniform and Turbulent Streams," *Journal of Fluid Mechanics*, Vol. 79, No. 2, 1977, pp. 307–335. doi:10.1017/S0022112077000172

[20] Healey, J. V., "The Prospects for Simulating the Helicopter-Ship Interface," *Naval Engineers Journal*, Vol. 99, No. 2, 1987, pp. 45–63. doi:10.1111/j.1559-3584.1987.tb02099.x

[21] Horn, J. F., Keller, J. D., Whitehouse, G. R., and McKillip, R. M., "An Analysis of Urban Airwake Effects on Heliport Flight Operations at the Chicago Children's Memorial Hospital," Illinois Department of Transportation, May 2011.

[22] Snyder, M. S., Kang, H.-S., Brownell, C. J., Luznik, L., Miklosovic, D. S., Burks, J. S., et al., "USNA Ship Air Wake Program Overview," 29th AIAA Applied Aerodynamics Conference, Honolulu, AIAA Paper 2011-3153, June 2011.

[23] Miklosovic, D. S., Snyder, M. R., and Kang, H.-S., "Ship Air Wake Wind Tunnel Test Results," *29th AIAA Applied Aerodynamics Conference*, Honolulu, AIAA Paper 2011-3155, June 2011.

[24] Roberson, F. D., and Snyder, M. R., "Ship Air Wake CFD Comparisons to Wind Tunnel and YP Boat Results," *29th AIAA Applied Aerodynamics Conference*, Honolulu, AIAA Paper 2011-3156, June 2011.

[25] Polsky, S. A., "A Computational Study of Unsteady Ship Airwake," *40th AIAA Aerospace Sciences Meeting and Exhibit*, Reno, NV, AIAA Paper 2002-1022, Jan. 2002.

[26] Bendat, J. S., and Piersol, A. G., *Random Data Analysis Procedures*, Wiley, New York, 1986, p. 566.

[27] Hoover, C., "Carrier Airflow Analysis—Smoke Tunnel and Full Scale Comparison of CVA-61," U.S. Naval Air Material Center, Rept. NAEF-ENG-6776, Philadelphia, 1961.

[28] Larose, G. L., and D'Auteuil, A., "On the Reynolds Number Sensitivity of the Aerodynamics of Bluff Bodies with Sharp Edges," *Journal of Wind Engineering and Industrial Aerodynamics*, Vol. 94, No. 5, 2006, pp. 365–376. doi:10.1016/j.jweia.2006.01.011

[29] Gaonkar, G. H., "Review of Turbulence Modeling and Related Applications to Some Problems of Helicopter Flight Dynamics," *Journal of the American Helicopter Society*, Vol. 53, No. 1, 2008, pp. 87–107. doi:10.4050/JAHS.53.87

[30] Zan, S. J., "Experimental Determination of Rotor Thrust in a Ship Airwake," *Journal of the American Helicopter Society*, Vol. 47, No. 2, 2002, pp. 100–108. doi:10.4050/JAHS.47.100

[31] Komerath, N. M., Smith, M. J., and Tung, C., "A Review of Rotor Wake Physics and Modeling," *Journal of the American Helicopter Society*, Vol. 56, No. 2, 2011, pp. 22006-1–22006-19.

[32] Lee, D., Sezer-Uzol, N., Horn, J. F., and Long, L. N., "Simulation of Helicopter Shipboard Launch and Recovery with Time-Accurate Airwakes," *Journal of Aircraft*, Vol. 42, No. 2, 2005, pp. 448–461. doi:10.2514/1.6786